

SCAM: A Real-World Typographic Robustness Evaluation for Multimodal Foundation Models

Justus Westerhoff^{1,2} Erblina Purrelku^{1,3}, Jakob Hackstein^{1,3}, Jonas Loos^{1,3}, Leo Pinetzki^{1,3}, Erik Rodner^{4,5}, Lorenz Hufe^{1,6}

¹BLISS e.V., ²Berliner Hochschule für Technik (BHT), ³Technische Universität Berlin, ⁴KI Werkstatt, Hochschule für Technik und Wirtschaft Berlin (HTW), ⁵Merantix Momentum, ⁶Fraunhofer Heinrich-Hertz-Institut, Berlin, Germany

Correspondence: justus.westerhoff@bht-berlin.de, lorenz.hufe@bliss.berlin

Reviewed on OpenReview: <https://openreview.net/forum?id=zCcJSErVHH>

Editor: Fernando Perez-Cruz

Abstract

Typographic attacks exploit the interplay between text and visual content in multimodal foundation models, causing misclassifications when misleading text is embedded within images. Existing datasets are limited in size and diversity, making it difficult to study such vulnerabilities. In this paper, we introduce SCAM, the largest and most diverse dataset of real-world typographic attack images to date, containing 1162 images across hundreds of object categories and attack words. Through extensive benchmarking of Vision-Language Models on SCAM, we demonstrate that typographic attacks significantly degrade performance, and identify that training data and model architecture influence the susceptibility to these attacks. Our findings indicate that typographic attacks remain effective against state-of-the-art Large Vision-Language Models, especially those employing vision encoders inherently vulnerable to such attacks. However, employing larger Large Language Model backbones reduces this vulnerability while simultaneously enhancing typographic understanding. Additionally, we demonstrate that synthetic attacks closely resemble real-world (handwritten) attacks, validating their use in research. Our work provides a comprehensive resource and empirical insights to facilitate future research toward robust and trustworthy multimodal AI systems. Finally, we publicly release the datasets introduced in this paper, along with the code for evaluations under www.bliss.berlin/research/scam.

Keywords: Typographic Attack Dataset, Vision-Language Models, Benchmarking

1 Introduction

Vision-Language Models (VLMs) such as CLIP (Radford et al., 2021) and SigLIP (Zhai et al., 2023) have demonstrated remarkable performance across various multimodal tasks (Gan et al., 2022), enabling applications in image classification (Radford et al., 2021; Menon and Vondrick, 2022), multimodal retrieval (Bogolin et al., 2022; Ming and Li, 2024), and generative tasks (Ramesh et al., 2022; Rombach et al., 2022; Gafni et al., 2022). However, recent research has revealed that these models are vulnerable to typographic attacks (Goh

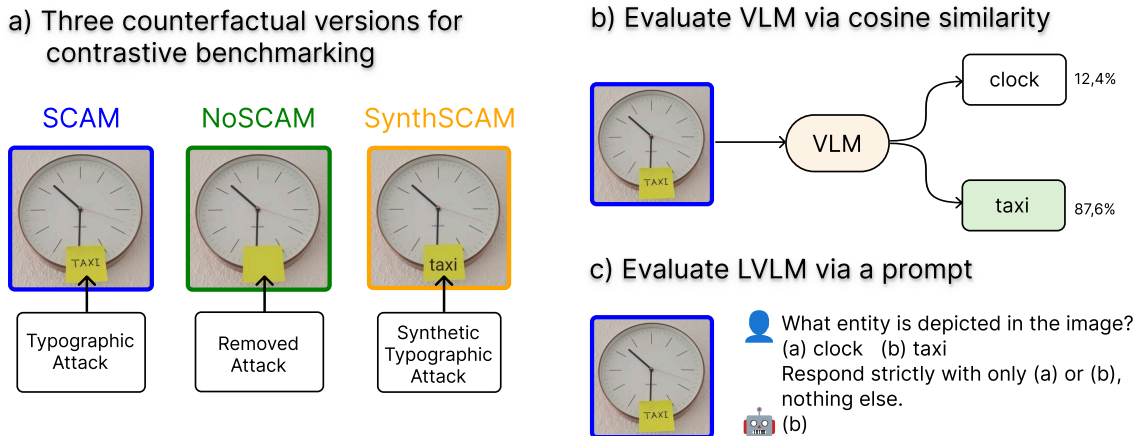


Figure 1: SCAM enables benchmarking safety-critical robustness to typographic attacks in multimodal models. a) We construct three image variants. Real-world attacks in SCAM, a cleaned baseline NoSCAM, and digitally simulated attacks in SynthSCAM allow causal evaluation of typographic vulnerabilities. b) VLMs are evaluated zero-shot by computing cosine similarity between image embeddings and textual labels. Our results show that misleading text embedded in images significantly shifts predictions, indicating overreliance on textual cues. c) LVLMs are assessed using prompt-based classification. Despite advanced architectures, models remain susceptible to typographic attacks in realistic user-facing tasks. Notably, synthetic attacks are as effective as real ones, validating their use for scalable robustness evaluation.

et al., 2021; Cheng et al., 2024c; Qraitem et al., 2024), which exploit the reliance on the textual component of multimodal learning.

Typographic attacks target multimodal foundation models by inserting human-readable text with misleading semantics into an image, leading to incorrect model predictions. Figure 1 depicts how adding the word “taxi” to an image of a “clock” can cause a model to misclassify it as a “taxi”. These attacks expose a fundamental interaction in multimodal learning: the model gets tricked by focusing on text within an image, more than the visual content itself. Understanding and mitigating such vulnerabilities is essential for the safe deployment of multimodal foundation models. With the growing use of VLMs in real-world applications, such as medical applications (Zhao et al., 2023; Li et al., 2023b; Hartsock and Rasool, 2024) and autonomous systems (Zhou et al., 2024), as well as in Large Vision-Language Models (LVLMs) (Liu et al., 2024c,a; Dubey et al., 2024), it is essential to ensure the safety and reliability of these models.

To facilitate research in this field, we introduce **S**ubtle **C**haracter **A**ttacks on **M**ultimodal **M**odels (SCAM), the largest and most diverse real-world typographic attack dataset to date. Each image contains an object with a semantically unrelated handwritten attack word¹ on a post-it note. Furthermore, we provide two variations, a clean dataset where attack words are removed (NoSCAM), and a synthetic dataset where attack words are digitally reintroduced (SynthSCAM).

1. While we use the term “word”, our attacks also incorporate phrases like “no left turn”.

In summary, we provide extensive evaluations over a range of VLMs and LVLMs and show that:

1. Models of both classes experience a significant drop in accuracy when faced with real-world typographic attacks (SCAM).
2. Synthetic attacks (SynthSCAM) closely align with real-world attacks, providing empirical support for the established practice of evaluating on synthetic datasets.
3. LVLMs, such as the LLaVA family, exhibit vulnerabilities to typographic attacks, reflecting weaknesses present in their vision encoders.
4. Employing larger Large Language Model (LLM) backbones reduces susceptibility to typographic attacks in LVLMs while also improving their typographic understanding.

2 Related Work

Multimodal Foundation Models. Multimodal pretraining, as established by CLIP (Radford et al., 2021) and SigLIP (Zhai et al., 2023), leverages image-text pairs to capture rich semantics suitable for a variety of applications (Dorbala et al., 2022; Zhou et al., 2023). This approach commonly features a contrastive objective to align visual and textual content in a shared latent space. Following this paradigm, various Vision-Language Models (VLMs) (Jia et al., 2021; Li et al., 2022; Tschannen et al., 2025) have been proposed, demonstrating impressive performance in numerous downstream tasks (Bogolin et al., 2022; Ramesh et al., 2022; Ming and Li, 2024). Recent research on Large Vision-Language Models (LVLMs) aligns the strong abilities of Large Language Models (LLMs) and vision encoders of VLMs to attain strong performance in vision-language tasks (Hurst et al., 2024; Liu et al., 2023b,a, 2024b; Team et al., 2025; Grattafiori et al., 2024; Meta, 2025; Anthropic, 2025).

Due to their strong capabilities and versatility, VLMs and LVLMs function as the backbone for a wide range of domains such as text-to-image generation (Rombach et al., 2022; Gafni et al., 2022).

Typographic Attacks. While vision-language pretraining enables strong performance, research has shown that VLMs and LVLMs are susceptible to typographic attacks (Goh et al., 2021; Cheng et al., 2024c; Qraitem et al., 2024). Existing works demonstrate several approaches to employ typographic attacks, for instance by Visual-Prompt-Injection (Kimura et al., 2024), with self-generated attacks (Qraitem et al., 2024), or in scene-coherent fashion (Cao et al., 2024b). Since VLMs are integrated into autonomous systems, typographic attacks are also known to occur in safety-critical applications such as autonomous driving (Chung et al., 2024).

Datasets. To study the intricacies of typographic attacks and evaluate the effectiveness of defense mechanisms, the majority of prior works (Gong et al., 2023; Cheng et al., 2024d,a,c; Qraitem et al., 2024; Kimura et al., 2024) synthetically add attack words into existing image datasets while only few (Ilharco et al., 2022; Materzyńska et al., 2022; Azuma and Matsui, 2023) propose datasets that exhibit real-world typographic attacks. Existing real-world datasets, such as PAINT (Ilharco et al., 2022) and Materzynska+(Materzyńska et al., 2022),

Table 1: Performance of VLMs and LVLMs available through OpenCLIP (OpenCLIP) resp. ollama (Ollama), and Anthropic’s resp. OpenAI’s API on the SCAM datasets. Note that internally all LLaVA models that we evaluate utilize ViT-L-14-336 trained by OpenAI for the image encoding. Furthermore, ViT-bigG-14 trained on laion2b is used in the Kandinsky diffusion model (Razzhigaev et al., 2023). This table presents a only selection of VLMs; the full list of all 99 can be found in table 6 in the appendix.

Model	Training data	Accuracy (%)		
		NoSCAM	SCAM	SynthSCAM
RN50	openai	97.76	36.61 ↓61.15	22.39 ↓75.37
ViT-B-32	laion2b	98.45	74.68 ↓23.77	56.16 ↓42.29
ViT-B-16	laion2b	98.71	69.16 ↓29.55	52.28 ↓46.43
ViT-B-16-SigLIP	webli	99.22	81.40 ↓17.82	75.45 ↓23.77
ViT-L-14	commonpool_xl	99.48	74.68 ↓24.80	68.56 ↓30.92
	openai	99.14	40.14 ↓59.00	26.61 ↓72.53
ViT-L-14-336	openai	99.22	33.85 ↓65.37	26.44 ↓72.78
ViT-L-14-CLIPA-336	datacomp1b	99.57	74.76 ↓24.81	65.81 ↓33.76
ViT-g-14	laion2b	99.05	61.93 ↓37.12	47.03 ↓52.02
ViT-bigG-14	laion2b	99.40	70.89 ↓28.51	58.91 ↓40.49
llava-llama3:8b	-	98.09	39.50 ↓58.59	44.04 ↓54.05
llava:7b-v1.6	-	97.50	58.43 ↓39.07	61.45 ↓36.06
llava:13b-v1.6	-	98.88	58.00 ↓40.88	55.42 ↓43.46
llava:34b-v1.6	-	98.97	84.85 ↓14.11	85.11 ↓13.86
gemma3:4b	-	97.24	58.05 ↓39.19	64.80 ↓32.44
gemma3:12b	-	99.14	52.02 ↓47.12	64.80 ↓34.34
gemma3:27b	-	97.42	81.67 ↓15.75	83.65 ↓13.77
llama3.2-vision:90b	-	98.88	71.01 ↓27.87	74.65 ↓24.22
llama4:scout	-	99.23	88.12 ↓11.10	87.18 ↓12.05
gpt-4o-mini-2024-07-18	-	99.40	84.68 ↓14.72	87.09 ↓12.31
claude-sonnet-4-20250514	-	99.31	91.13 ↓8.18	90.28 ↓9.03
gpt-4o-2024-08-06	-	99.48	96.82 ↓2.67	94.58 ↓4.90

lack the diversity and scale needed to reliably evaluate the vulnerabilities of multimodal foundation models. The previously largest real-world typographic attack dataset, RTA-100 (Azuma and Matsui, 2023), consists of 1000 images spanning 100 objects and attack words. However, these existing real-world datasets remain limited in both scale and diversity, restricting their ability to comprehensively assess the vulnerabilities of multimodal foundation models (see table 2 for a comparison, and section A.2 for example images of PAINT and RTA-100). Our dataset addresses this limitation by introducing substantially larger variability across object–word combinations, which mitigates dataset bias and enables a more reliable assessment of generalization in VLMs and LVLMs. Furthermore, current datasets lack a structured comparison between real-world and synthetic typographic attacks, preventing a systematic analysis of transferability between these domains. SCAM is the first dataset



Figure 2: Cropped examples from the **Subtle Character Attacks on Multimodal Models (SCAM)** dataset, illustrating the natural variability introduced by nine different contributors using distinct smartphones, handwriting styles, and recording environments. This diversity results in variations in lighting, camera quality, backgrounds, and writing appearance. Additional uncropped examples for both NoSCAM and SynthSCAM are provided in fig. 7 in the appendix.

to provide three explicitly aligned components: (i) SCAM, containing real-world attacked scenes, (ii) NoSCAM, the corresponding clean counterparts of the exact same scenes, and (iii) SynthSCAM, synthetically manipulated versions of the same object–word pairs. This tri-part design enables precise, controlled measurement of typographic attack effects and systematic comparisons across clean, real, and synthetic domains, establishing a stronger foundation for rigorous evaluation of VLMs and LVLMs as well as the development of effective defense mechanisms.

3 SCAM Dataset

We introduce **Subtle Character Attacks on Multimodal Models (SCAM)**, the largest and most diverse real-world typographic attack dataset to date, containing 1162 images (see table 2). The dataset and its two variations (NoSCAM and SynthSCAM), enabling empirical assessment of transferability between these settings, are publicly available on Hugging Face together with the fully compatible and publicly accessible SCAM benchmark repository for standardized evaluation.

Data Collection. SCAM was collaboratively constructed by nine contributors using nice different smartphones, ensuring natural variation in image quality. The data were recorded across diverse indoor and outdoor environments, including households, utility stores, and traffic infrastructure, under heterogeneous lighting conditions and viewing angles. This variability, illustrated in fig. 2, reflects real-world conditions more faithfully than prior datasets.

Each image in the SCAM dataset captures a physical object together with an unrelated attack word handwritten in English on a single post-it note and placed next to the object, as shown in fig. 1a. Sticky notes were deliberately chosen as the attack medium because they are common in everyday contexts (e.g., labeling in offices, classrooms, and shops) and provide a realistic, reproducible surface for typographic attacks.

To create the cleaned NoSCAM dataset, we remove all attack words by overlaying the post-it notes with their original color, thereby obscuring the text while preserving the original object images. This provides clean, paired counterparts for every attacked image. Additionally, we create the synthetic SynthSCAM dataset by reintroducing the original attack words into the images (using the **Roboto** font), matching the color of the ink from the original images. Choosing a uniform font style in this synthetic variant was a deliberate simplification. Prior synthetic attack datasets have already explored variations in font position, opacity, and color (Cheng et al., 2024a), whereas our focus is on providing clean, attacked, and synthetic counterparts of the same scenes.

Data Annotation and Processing. All images were manually annotated with object and attack word labels as well as post-it size (in %) as part of a voluntary community effort. The annotation process was conducted using Label Studio (Studio). To standardize the dataset, all images were zero-padded and downscaled to 512×512 pixels using `cv2.INTER_AREA` (OpenCV), an interpolation method that preserves details while minimizing distortion.

Dataset Statistics. SCAM comprises 1162 images, featuring 660 distinct object labels and 206 unique attack words, that form 1,147 unique object-word combinations. The complete lists of objects and attack words are provided in section A.9. We categorize the attack words into ten groups, covering both everyday words and safety-critical terms – such as “pedestrian” or “no left turn” – that are essential for autonomous driving systems. The distribution of these groups is depicted in fig. 3.

As summarized in table 2, SCAM significantly surpasses existing real-world datasets in diversity, both in terms of object counts and attack words. Compared to RTA-100 (Azuma and Matsui, 2023), SCAM covers a much broader range of objects (660 vs. 100) and attack words (206 vs. 100), offering a more comprehensive evaluation of model robustness to typographic attacks. The three explicitly aligned components – SCAM, NoSCAM, and SynthSCAM – allow precise, controlled measurement of typographic attack effects and direct comparisons between clean, real, and synthetic conditions, thereby closing critical gaps in prior datasets.

Maintenance and Ethical Use. SCAM is publicly hosted on Hugging Face under a stable organization account². The dataset card provides versioning, update logs, and contact

2. <https://huggingface.co/datasets/BLISS-e-V/SCAM>

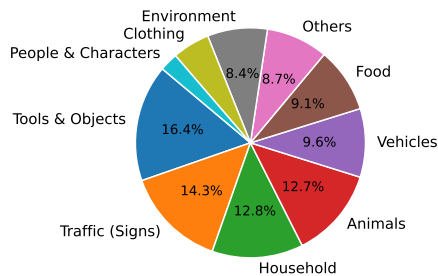


Figure 3: Distribution of attack words in SCAM into categories, highlighting both everyday terms and safety-critical vocabulary.

Table 2: Comparison of real-world typographic attack datasets. SCAM is much more diverse in terms of objects and attack words.

Dataset	Images	Objects	Attacks
PAINT (Ilharco et al., 2022)	110	89	87
Materzynska+ (Materzyńska et al., 2022)	180	20	8
RTA-100 (Azuma and Matsui, 2023)	1000	100	100
SCAM (ours)	1162	660	206

information, and we will maintain SCAM by releasing documented updates if errors are discovered or extensions are added. Users can contact the corresponding authors to report issues, request corrections, or raise takedown concerns.

All images in SCAM depict everyday objects with handwritten English words on post-it notes. SCAM does not contain personal, biometric, or otherwise sensitive data. The dataset is released for research purposes under the license specified on the dataset card, and users are expected to follow standard citation practices and refrain from deploying models trained on SCAM in applications intended to harm or deceive humans. A more detailed discussion of potential risks and benefits is provided in the Broader Impact Statement on page 13.

4 Evaluation

We evaluate VLMs on a zero-shot classification task and LLMs in a generative prompt-based classification setup. Both evaluations are conducted on the SCAM datasets (SCAM, NoSCAM, SynthSCAM) and additionally on PAINT (Ilharco et al., 2022) and RTA-100 (Azuma and Matsui, 2023). The evaluation aims to demonstrate how typographic attacks, whether real-world or synthetic, affect the accuracy of multimodal foundation models in correctly predicting the object (rather than the attack word) depicted in the image.

Experimental Setup. To evaluate VLMs such as CLIP (Radford et al., 2021) and SigLIP (Zhai et al., 2023), we use the OpenCLIP suite (Ilharco et al., 2021; Schuhmann et al., 2022; Radford et al., 2021; Cherti et al., 2023; OpenCLIP). We also evaluate eleven LLMs, including Claude Sonnet 4 (Anthropic, 2025), GPT-4o (Hurst et al., 2024), LLaVA (Liu et al., 2023b,a, 2024b), Gemma3 (Team et al., 2025), Llama3.2-vision (Grattafiori et al., 2024) and Llama4 (Meta, 2025) models. The LLaVA, Gemma3, and Llama models are deployed via the Ollama platform (Ollama), whereas Claude Sonnet 4 and GPT-4o is accessed via OpenAI’s resp. Anthropic’s API. An overview of selected models is provided in table 1, while table 6 presents the complete list of all 111 evaluated models.

Evaluating VLMs. We evaluate the performance of VLMs in a zero-shot classification task. For each image, we compute the cosine similarity between its embedding and the text embeddings of both the object label and the attack word. These text embeddings are generated using the set of text templates proposed in (Radford et al., 2021), as detailed in section A.3. The predicted label is then determined based on the highest cosine similarity score. An overview of this process is depicted in fig. 1b. Here, when the model is presented with an image of a “clock” with the attack word “taxi”, it does not classify the image correctly. All evaluations of VLMs were performed on an A100 40GB card.

Evaluating LVLMs. To assess the robustness of an LVLM against typographic attacks, we evaluate whether its output changes when exposed to typographic modifications. Our evaluation follows the setup illustrated in fig. 1c, inspired by (Cheng et al., 2024b). The model is provided with an image along with the following prompt:

```
What entity is depicted in the image?
(a) clock
(b) taxi
Respond strictly with only (a) or (b),
nothing else.
```

In this setup, the model correctly outputs “(a)” (the object label) when no attack word is present, as in the NoSCAM dataset. However, when the attack word is included, the model changes its response to “(b)”.

Note that we randomly alternate between (a) and (b) as the object label to eliminate positional or ordering biases in the prompt. In fewer than 1% of cases, the generated answer does not conform to the expected format (that is, `answer.lower()` is not contained in `{“a”, “a)”, “a:” “a]”, “a.”, “(a)”, “b”, “b)”, “b:” “b]”, “b.”, “(b)”, f“{object label}”, f“{attack label}”}`). Furthermore, we analyze the effect of varying the exact prompt in section A.6.

All LLaVA and Gemma3 models were evaluated on an A100 40GB card, and `llama3.2-vision:90b` and `llama4:scout` on an H100 80GB.

Table 3: Alignment between real-world (SCAM) and synthetic (SynthSCAM) attacks. The tables present average confusion matrices. The similarity in outcomes indicates that synthetic attacks closely replicate the effects of real attacks. Values represent the mean \pm standard deviation, rounded to integers.

	(a) Average across all VLMs with over 90% accuracy on NoSCAM.		(b) Average across all LVLMs.	
	SynthSCAM fails	SynthSCAM succeeds	SynthSCAM fails	SynthSCAM succeeds
SCAM fails	648 \pm 192	154 \pm 68	SCAM fails	741 \pm 243
SCAM succeeds	18 \pm 11	341 \pm 151	SCAM succeeds	124 \pm 71
				201 \pm 137

5 Results

We demonstrate that multimodal foundation models are susceptible to typographic attacks in real-world data, as shown in table 1. Our results show that typographic attacks on VLMs lead to an average drop in accuracy of 26 percentage points. LLMs exhibit similar behavior, with the choice of vision encoder appearing to influence the extent of accuracy degradation. Furthermore, our analysis reveals that typographic attacks in real-world and synthetic data similarly affect model accuracy, as demonstrated by the accuracy distributions in fig. 4 and the alignment between SCAM and SynthSCAM reflected in the confusion matrices in table 3. These results show that synthetic typographic attacks closely mirror real-world scenarios, making them a reliable proxy for evaluating the robustness of multimodal foundation models.

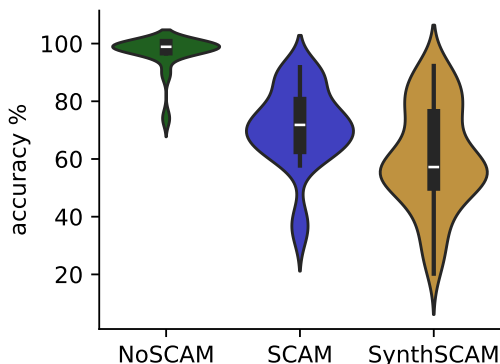


Figure 4: Accuracy distribution of 99 VLMs across NoSCAM, SCAM, and SynthSCAM datasets. SCAM effectively lowers accuracy, and its similarity to SynthSCAM suggests synthetic attacks replicate real ones. Table 6 in the appendix provides a full list of models and their accuracies.

Table 4: Training dataset choice significantly affects accuracy, as shown by the results on SCAM for the model ViT-B-16 trained by the OpenCLIP team on different datasets.

Dataset	Accuracy %
commonpool_1_text	91.82
commonpool_1_image	90.96
commonpool_1_basic	90.09
commonpool_1	88.72
datacomp_1	80.10
commonpool_1_laion	79.24
commonpool_1_clip	71.15
laion2b	69.16
laion400m	69.04
datacomp_xl	68.39

Zero-Shot Results for VLMs. As shown in fig. 4, VLMs achieve high prediction accuracy in the zero-shot classification task on the NoSCAM dataset. However, accuracy declines for almost all models when evaluated on the SCAM and SynthSCAM datasets. Specifically, accuracy on SCAM drops by approximately 26 percentage points on average, while the SynthSCAM dataset exhibits an even steeper decline of 36 percentage points. For a detailed breakdown of model accuracies across the three datasets, see table 6 in the appendix.

Impact of Training Dataset and Model Architecture. We investigate the vulnerability of VLMs by examining the impact of their training data, training paradigm, and model architecture, on their susceptibility to typographic attacks.

Table 4 presents the impact of training data on the ViT-B models (Dosovitskiy et al., 2020) trained by the OpenCLIP team. We focus solely on these models as they share the same training paradigm but are trained on different datasets. Overall, the ViT-B models trained on the LAION datasets (Schuhmann et al., 2022) are highly susceptible to typographic attacks,

Table 5: VLMs’ architecture impacts susceptibility to typographic attacks. SigLIP outperforms CLIP, ViT outperforms ResNets, and ViTs become more susceptible to typographic attacks as patch size decreases. The tables present (average) accuracy (Acc.) % on SCAM.

(a) Average across different CLIP and SigLIP models trained by OpenAI and Visheratin (2023) on LAION-COCO NLLB (referred to, in OpenCLIP, as v1). More details about the selection process can be found in section A.5.			(b) Dataset fixed to laion2b.		
Training data	Architecture	Acc. %	Model	Patch Size	Acc. %
openai	CLIP-ViT	43.63	ViT-B-32	32	74.68
	CLIP-RN	35.76	ViT-bigG-14	14	70.89
v1	SigLIP-ViT	75.80	ViT-B-16	16	69.16
	CLIP-ViT	69.04	ViT-H-14	14	62.96
			ViT-L-14	14	62.53
			ViT-g-14	14	61.93

while certain CommonPool variants (Gadre et al., 2023) exhibit lower vulnerability, such as the `text` and `image` filtered datasets, generated based on textual and visual overlaps with ImageNet classes, respectively. Notably, the vulnerable `commonpool_1_clip` dataset results from selecting data points based on cosine similarity scores computed from image and text embeddings produced by the pretrained ViT-L-14 (Radford et al., 2021) model from OpenAI. Consequently, as indicated by the accuracies for that model in table 1, this filtering criterion appears to propagate susceptibility.

While training data significantly affects robustness, it is equally important to understand how the model architecture impacts typographic attack resistance. We compare different architectures: CLIP-RN (ResNets (He et al., 2016)) and CLIP-ViT models trained by OpenAI (Radford et al., 2021), as well as CLIP-ViT and SigLIP-ViT models trained on LAION-COCO NLLB (Visheratin, 2023) (see table 5a). Our findings show that, on average, CLIP-ViT models exhibit greater resilience to typographic attacks compared to CLIP-RN models. Similarly, SigLIP-ViT shows increased robustness compared to CLIP-ViT.

Moreover, our evaluations show that the robustness of VLMs against typographic attacks varies with patch size, as illustrated in table 5b. Notably, smaller patch sizes generally result in higher susceptibility to typographic attacks.

Lastly, fig. 5 shows that there is no noticeable correlation between model size and accuracy drop caused by typographic attacks. However, we find that the original CLIP models (Radford et al., 2021) trained by OpenAI perform significantly worse across all sizes.

Impact of the Size of the Attack. We observe a strong correlation between zero-shot accuracy and post-it area, indicating that the size of the attack text affects accuracy (see fig. 6). The mean accuracy across all models follows this trend, which is consistent with the findings in (Cheng et al., 2024a).

Prompt-Based Classification Results for LVLMs. Our evaluation highlights an important finding: while LVLMs are vulnerable to typographic attacks (see table 1), their susceptibility appears to be influenced by the strength of the underlying vision encoder. Smaller LLaVA and Gemma3 models, such as `gemma3:4b`, `llava:7b-v1.6`, `llava-llama3:8b`,

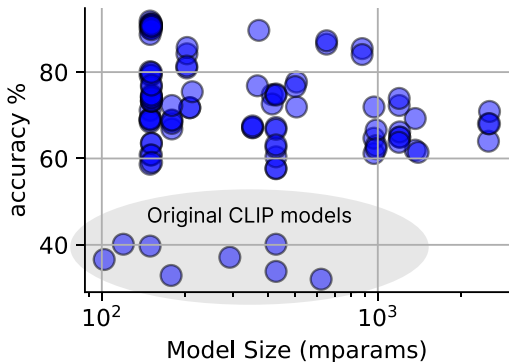


Figure 5: Susceptibility to typographic attack (accuracy on SCAM) is agnostic of VLM size, measured in millions of parameters.

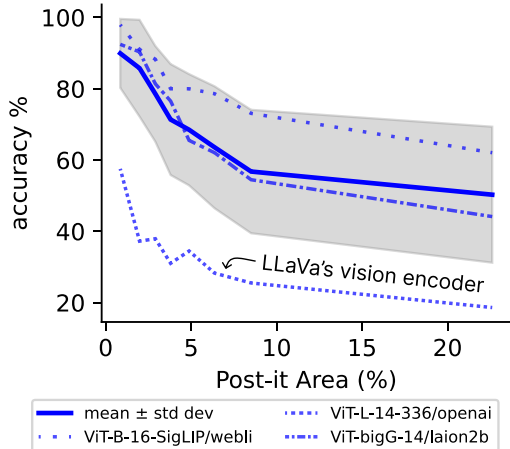


Figure 6: Model accuracy on SCAM decreases as the post-it area increases. Shaded area shows mean \pm standard deviation across all 99 VLMs that we evaluate.

`gemma3:12b`, and `llava:13b-v1.6`, suffer substantial accuracy drops of more than 40-60 percentage points under typographic attacks. We hypothesize that this vulnerability stems from their reliance on weaker vision encoders, particularly the ViT-L-14-336 backbone trained by OpenAI, which is highly susceptible to such attacks (see fig. 6). However, as model size increases, the robustness to typographic attacks improves. Models with larger LLM backbones, such as `gemma:27b` and `llava:34b-v1.6`, exhibit significantly better performance under attack. This suggests that a more powerful LLM backbone can compensate for the limitations of the vision encoder, making these models more resilient to typographic distortions. In comparison, presumably much larger closed-source models such as `claude-sonnet-4-20250514` and `gpt-4o` exhibit strong robustness to typographic attacks, with a minimal accuracy drop of around 8 resp. 3 percentage points. The smaller `gpt-4o-mini` and `llama4:scout`, however, experience a higher drop of approximately 15 points, illustrating again that larger models tend to be more robust. Despite that, model size alone does not determine robustness. In fact, the large `llama3.2-vision:90b` model is more vulnerable to typographic attacks than the smaller `llava:34b-v1.6`. These results highlight that while vision encoders remain a critical vulnerability, increasing the size and quality of the LLM backbone plays a key role in reducing susceptibility to typographic attacks.

Impact of VLM and LLM Size on LVLM Performance. Section A.7 presents a preliminary experiment that isolates the role of the vision encoder in LVLMs with respect to typographic robustness. The experiment does not show a clear gain in robustness when substituting the vision encoder with one ranked safer by SCAM, while keeping the LLM, training data, and training regime unchanged. Instead, the overall performance decreases, highlighting the difficulty of choosing the optimal vision encoder and showcasing the need for further experiments investigating the robustness impact of different VLM choices. Apart

from that, as discussed in section A.8, scaling up the LLM backbone not only improves performance on SCAM but also enhances the model’s general typographic understanding on textual and OCR-based benchmarks.

6 Discussion

Our evaluations on the **Subtle Character Attacks on Multimodal Models** (SCAM) datasets confirm previous findings (Goh et al., 2021; Cheng et al., 2024c; Qraitem et al., 2024) that multimodal foundation models remain vulnerable to typographic attacks, whether real-world (SCAM) or synthetic (SynthSCAM). Notably, we find that synthetic attacks are just as effective as real-world ones, leading to comparable performance drops.

Our analysis further reveals that training regime, training data, and model architecture significantly influence susceptibility of Vision-Language Models (VLMs) to typographic attacks, whereas model size alone does not correlate with robustness. In Large Vision-Language Models (LVLMs), vulnerability to typographic attacks appears to carry over from the vision encoder, making these models susceptible to the same weaknesses. However, we find that larger Large Language Model (LLM) backbones can mitigate this effect, leading to improved robustness and accuracy to typographic attacks, while also improving their typographic understanding.

Limitations. Despite incorporating a different, “safer” prompt in section A.6, a central limitation of our evaluation remains the reliance on “naive prompting” (He et al., 2024; Cao et al., 2024a) for assessing LVLMs. More advanced multi-prompt evaluation strategies may yield a more reliable measure of robustness against typographic attacks. A further limitation is our exclusive focus on English-language attacks; future work should investigate whether language-specific factors influence model susceptibility..

Future Work. As multimodal models are increasingly deployed to safety-critical applications (Li et al., 2023b; Hartsock and Rasool, 2024; Zhou et al., 2024), ensuring robustness against typographic attacks is essential to prevent serious consequences. Approaches such as alignment training (Afzali et al., 2024) or (mechanistic) defense techniques (Azuma and Matsui, 2023; Hufe et al., 2025) offer promising directions for enhancing robustness. The aligned NoSCAM/SCAM pairs are well-suited for causal and mechanistic analyses, as they allow for controlled interventions while keeping scene semantics fixed. We view SCAM primarily as a dataset and benchmark to support such work and expect future research to leverage this alignment to develop and evaluate mechanistic defenses against typographic attacks. Furthermore, our evaluations suggest that the vulnerability of LVLMs to typographic attacks is tied to their vision encoder. However, our initial experiments (section A.7) show that simply swapping LLaVA’s vision encoder for a more robust one does not reliably transfer robustness when integrated naively. Future work will extend this by systematically retraining LLaVA models with a range of vision backbones to evaluate their role in attack susceptibility and to assess whether encoder strength alone suffices or if additional adaptation steps are necessary.

7 Conclusion

In this paper, we introduced the **Subtle Character Attacks on Multimodal Models (SCAM)** dataset (and two variations, NoSCAM and SynthSCAM), the largest and most diverse collection of real-world images designed to evaluate the vulnerability of multimodal foundation models to typographic attacks. Our evaluation demonstrated that current state-of-the-art multimodal models are significantly affected by typographic attacks, highlighting a critical weakness in their robustness. We expect that our broad analysis of Vision-Language Models (VLMs) and Large Vision-Language Models (LVLMs) will help researchers make more informed choices when selecting typographically robust models for their safety-critical downstream applications.

Broader Impact Statement

Our work highlights a concrete vulnerability in (Large) Vision-Language Models: typographic attacks that cause models to overly rely on embedded text rather than visual content. This vulnerability has clear negative implications. Malicious actors could exploit our findings to systematically uncover weaknesses in deployed vision-language systems, using typographic cues to mislead models in safety-critical settings such as medical decision support, navigation, or content moderation. By releasing a large and diverse dataset of such attacks, we also create the possibility that others could study these loopholes with the explicit aim of designing more effective attacks.

At the same time, we believe the benefits for research and defense outweigh these risks. Robustness research requires shared realistic benchmarks and reproducible baselines. SCAM provides a standardized resource that allows the community to evaluate typographic vulnerabilities and compare defense methods systematically, and to study how training data and model design affect susceptibility. By demonstrating that synthetic attacks reliably mirror real-world ones, we also reduce the need for ongoing collection of handwritten adversarial examples, lowering barriers for future research.

Acknowledgments and Disclosure of Funding

Our work is funded by the Deutsche Forschungsgemeinschaft (DFG, German Research Foundation) Project-ID 528483508 - FIP 12. We thank the BLISS³ community – its very existence, collaborative energy, and shared commitment to open research made this work possible. Special thanks to Zeynep Altayli, Philippa Ringe, and Joseph Tschörner for their valuable efforts in image collection and labeling.

Author Contributions

JW was responsible for image processing, code development, model evaluations, visualizations, and overall coordination. EP contributed to conceptualization, figure design, and manuscript writing, including the introduction, dataset, evaluation, and drafted most of the results and discussion sections. JH focused on related work research and supported overall writing.

3. <https://bliss.berlin/>

JL supported model evaluations, managed data and code hosting, and created the project webpage. LP contributed to dataset expansion through large-scale labeling and provided continuous critical feedback. EH provided supervision and contributed through discussions. LH initiated the project, provided supervision throughout, designed the data collection protocol, and guided the conceptual and methodological direction of the work. All authors except EH contributed to image collection and labeling.

References

- Amirabbas Afzali, Borna Khodabandeh, Ali Rasekh, Mahyar JafariNodeh, Simon Gottschalk, et al. Aligning visual contrastive learning models via preference optimization. *arXiv preprint arXiv:2411.08923*, 2024.
- Anthropic. Claude opus 4 & claude sonnet 4 — system card. <https://www-cdn.anthropic.com/6d8a8055020700718b0c49369f60816ba2a7c285.pdf>, 2025.
- Hiroki Azuma and Yusuke Matsui. Defense-prefix for preventing typographic attacks on clip. In *Proceedings of the IEEE/CVF International Conference on Computer Vision*, pages 3644–3653, 2023.
- Simion-Vlad Bogolin, Ioana Croitoru, Hailin Jin, Yang Liu, and Samuel Albanie. Cross modal retrieval with querybank normalisation. In *Proceedings of the IEEE/CVF Conference on Computer Vision and Pattern Recognition*, pages 5194–5205, 2022.
- Bowen Cao, Deng Cai, Zhisong Zhang, Yuexian Zou, and Wai Lam. On the worst prompt performance of large language models. *arXiv preprint arXiv:2406.10248*, 2024a.
- Yue Cao, Yun Xing, Jie Zhang, Di Lin, Tianwei Zhang, Ivor Tsang, Yang Liu, and Qing Guo. Scenetap: Scene-coherent typographic adversarial planner against vision-language models in real-world environments. *arXiv preprint arXiv:2412.00114*, 2024b.
- Hao Cheng, Erjia Xiao, Jindong Gu, Le Yang, Jinhao Duan, Jize Zhang, Jiahang Cao, Kaidi Xu, and Renjing Xu. Unveiling typographic deceptions: Insights of the typographic vulnerability in large vision-language models. In *European Conference on Computer Vision*, pages 179–196. Springer, 2024a.
- Hao Cheng, Erjia Xiao, and Renjing Xu. Typographic attacks in large multimodal models can be alleviated by more informative prompts. *arXiv e-prints*, pages arXiv–2402, 2024b.
- Hao Cheng, Erjia Xiao, Jiayan Yang, Jiahang Cao, Qiang Zhang, Le Yang, Jize Zhang, Kaidi Xu, Jindong Gu, and Renjing Xu. Typography leads semantic diversifying: Amplifying adversarial transferability across multimodal large language models. *arXiv preprint arXiv:2405.20090*, 2024c.
- Hao Cheng, Erjia Xiao, Jiayan Yang, Jiahang Cao, Qiang Zhang, Jize Zhang, Kaidi Xu, Jindong Gu, and Renjing Xu. Uncovering vision modality threats in image-to-image tasks. *arXiv preprint arXiv:2412.05538*, 2024d.
- Mehdi Cherti, Romain Beaumont, Ross Wightman, Mitchell Wortsman, Gabriel Ilharco, Cade Gordon, Christoph Schuhmann, Ludwig Schmidt, and Jenia Jitsev. Reproducible scaling laws for contrastive language-image learning. In *Proceedings of the IEEE/CVF Conference on Computer Vision and Pattern Recognition*, pages 2818–2829, 2023.

- Nhat Chung, Sensen Gao, Tuan-Anh Vu, Jie Zhang, Aishan Liu, Yun Lin, Jin Song Dong, and Qing Guo. Towards transferable attacks against vision-llms in autonomous driving with typography. *arXiv preprint arXiv:2405.14169*, 2024.
- Vishnu Sashank Dorbala, Gunnar Sigurdsson, Robinson Piramuthu, Jesse Thomason, and Gaurav S Sukhatme. Clip-nav: Using clip for zero-shot vision-and-language navigation. *arXiv preprint arXiv:2211.16649*, 2022.
- Alexey Dosovitskiy, Lucas Beyer, Alexander Kolesnikov, Dirk Weissenborn, Xiaohua Zhai, Thomas Unterthiner, Mostafa Dehghani, Matthias Minderer, Georg Heigold, Sylvain Gelly, et al. An image is worth 16x16 words: Transformers for image recognition at scale. *arXiv preprint arXiv:2010.11929*, 2020.
- Haodong Duan, Junming Yang, Yuxuan Qiao, Xinyu Fang, Lin Chen, Yuan Liu, Xiaoyi Dong, Yuhang Zang, Pan Zhang, Jiaqi Wang, et al. Vlmevalkit: An open-source toolkit for evaluating large multi-modality models. In *Proceedings of the 32nd ACM International Conference on Multimedia*, pages 11198–11201, 2024.
- Abhimanyu Dubey, Abhinav Jauhri, Abhinav Pandey, Abhishek Kadian, Ahmad Al-Dahle, Aiesha Letman, Akhil Mathur, Alan Schelten, Amy Yang, Angela Fan, et al. The llama 3 herd of models. *arXiv preprint arXiv:2407.21783*, 2024.
- Chaoyou Fu, Peixian Chen, Yunhang Shen, Yulei Qin, Mengdan Zhang, Xu Lin, Jinrui Yang, Xiawu Zheng, Ke Li, Xing Sun, et al. Mme: A comprehensive evaluation benchmark for multimodal large language models. *arXiv preprint arXiv:2306.13394*, 2023.
- Samir Yitzhak Gadre, Gabriel Ilharco, Alex Fang, Jonathan Hayase, Georgios Smyrnis, Thao Nguyen, Ryan Marten, Mitchell Wortsman, Dhruva Ghosh, Jieyu Zhang, et al. Datacomp: In search of the next generation of multimodal datasets. *Advances in Neural Information Processing Systems*, 36: 27092–27112, 2023.
- Oran Gafni, Adam Polyak, Oron Ashual, Shelly Sheynin, Devi Parikh, and Yaniv Taigman. Make-a-scene: Scene-based text-to-image generation with human priors. In *European Conference on Computer Vision*, pages 89–106. Springer, 2022.
- Zhe Gan, Linjie Li, Chunyuan Li, Lijuan Wang, Zicheng Liu, Jianfeng Gao, et al. Vision-language pre-training: Basics, recent advances, and future trends. *Foundations and Trends® in Computer Graphics and Vision*, 14(3–4):163–352, 2022.
- Gabriel Goh, Nick Cammarata, Chelsea Voss, Shan Carter, Michael Petrov, Ludwig Schubert, Alec Radford, and Chris Olah. Multimodal neurons in artificial neural networks. *Distill*, 2021. doi: 10.23915/distill.00030. <https://distill.pub/2021/multimodal-neurons>.
- Yichen Gong, DeLong Ran, Jinyuan Liu, Conglei Wang, Tianshuo Cong, Anyu Wang, Sisi Duan, and Xiaoyun Wang. Figstep: Jailbreaking large vision-language models via typographic visual prompts. *arXiv preprint arXiv:2311.05608*, 2023.
- Aaron Grattafiori, Abhimanyu Dubey, Abhinav Jauhri, Abhinav Pandey, Abhishek Kadian, Ahmad Al-Dahle, Aiesha Letman, Akhil Mathur, Alan Schelten, Alex Vaughan, et al. The llama 3 herd of models. *arXiv preprint arXiv:2407.21783*, 2024.
- Iryna Hartsock and Ghulam Rasool. Vision-language models for medical report generation and visual question answering: A review. *Frontiers in Artificial Intelligence*, 7:1430984, 2024.

- Jia He, Mukund Rungta, David Koleczek, Arshdeep Sekhon, Franklin X Wang, and Sadid Hasan. Does prompt formatting have any impact on llm performance? *arXiv preprint arXiv:2411.10541*, 2024.
- Kaiming He, Xiangyu Zhang, Shaoqing Ren, and Jian Sun. Deep residual learning for image recognition. In *Proceedings of the IEEE conference on computer vision and pattern recognition*, pages 770–778, 2016.
- Lorenz Hufe, Constantin Venhoff, Maximilian Dreyer, Sebastian Lopuschkin, and Wojciech Samek. Towards mechanistic defenses against typographic attacks in clip. *arXiv preprint arXiv:2508.20570*, 2025.
- Aaron Hurst, Adam Lerer, Adam P Goucher, Adam Perelman, Aditya Ramesh, Aidan Clark, AJ Ostrow, Akila Welihinda, Alan Hayes, Alec Radford, et al. Gpt-4o system card. *arXiv preprint arXiv:2410.21276*, 2024.
- Gabriel Ilharco, Mitchell Wortsman, Ross Wightman, Cade Gordon, Nicholas Carlini, Rohan Taori, Achal Dave, Vaishaal Shankar, Hongseok Namkoong, John Miller, Hannaneh Hajishirzi, Ali Farhadi, and Ludwig Schmidt. Openclip, 2021. URL <https://doi.org/10.5281/zenodo.5143773>. If you use this software, please cite it as below.
- Gabriel Ilharco, Mitchell Wortsman, Samir Yitzhak Gadre, Shuran Song, Hannaneh Hajishirzi, Simon Kornblith, Ali Farhadi, and Ludwig Schmidt. Patching open-vocabulary models by interpolating weights. *Advances in Neural Information Processing Systems*, 35:29262–29277, 2022.
- Chao Jia, Yinfei Yang, Ye Xia, Yi-Ting Chen, Zarana Parekh, Hieu Pham, Quoc Le, Yun-Hsuan Sung, Zhen Li, and Tom Duerig. Scaling up visual and vision-language representation learning with noisy text supervision. In *International conference on machine learning*, pages 4904–4916. PMLR, 2021.
- Subaru Kimura, Ryota Tanaka, Shumpei Miyawaki, Jun Suzuki, and Keisuke Sakaguchi. Empirical analysis of large vision-language models against goal hijacking via visual prompt injection. *arXiv preprint arXiv:2408.03554*, 2024.
- Bohao Li, Rui Wang, Guangzhi Wang, Yuying Ge, Yixiao Ge, and Ying Shan. Seed-bench: Benchmarking multimodal llms with generative comprehension. *arXiv preprint arXiv:2307.16125*, 2023a.
- Chunyuan Li, Cliff Wong, Sheng Zhang, Naoto Usuyama, Haotian Liu, Jianwei Yang, Tristan Naumann, Hoifung Poon, and Jianfeng Gao. Llava-med: Training a large language-and-vision assistant for biomedicine in one day. *Advances in Neural Information Processing Systems*, 36: 28541–28564, 2023b.
- Junnan Li, Dongxu Li, Caiming Xiong, and Steven Hoi. Blip: Bootstrapping language-image pre-training for unified vision-language understanding and generation. In *International conference on machine learning*, pages 12888–12900. PMLR, 2022.
- Xianhang Li, Zeyu Wang, and Cihang Xie. An inverse scaling law for clip training. In *NeurIPS*, 2023c.
- Xianhang Li, Zeyu Wang, and Cihang Xie. Clipa-v2: Scaling clip training with 81.1 *arXiv preprint arXiv:2306.15658*, 2023d.
- Yifan Li, Hangyu Guo, Kun Zhou, Wayne Xin Zhao, and Ji-Rong Wen. Images are achilles’ heel of alignment: Exploiting visual vulnerabilities for jailbreaking multimodal large language models. In *European Conference on Computer Vision*, pages 174–189. Springer, 2024.

- Haotian Liu. <https://github.com/haotian-liu/LLaVA>.
- Haotian Liu, Chunyuan Li, Yuheng Li, and Yong Jae Lee. Improved baselines with visual instruction tuning, 2023a.
- Haotian Liu, Chunyuan Li, Qingyang Wu, and Yong Jae Lee. Visual instruction tuning, 2023b.
- Haotian Liu, Chunyuan Li, Yuheng Li, and Yong Jae Lee. Improved baselines with visual instruction tuning. In *Proceedings of the IEEE/CVF Conference on Computer Vision and Pattern Recognition*, pages 26296–26306, 2024a.
- Haotian Liu, Chunyuan Li, Yuheng Li, Bo Li, Yuanhan Zhang, Sheng Shen, and Yong Jae Lee. Llava-next: Improved reasoning, ocr, and world knowledge, 2024b. URL <https://llava-vl.github.io/blog/2024-01-30-llava-next/>.
- Haotian Liu, Chunyuan Li, Qingyang Wu, and Yong Jae Lee. Visual instruction tuning. *Advances in neural information processing systems*, 36, 2024c.
- Yuliang Liu, Zhang Li, Mingxin Huang, Biao Yang, Wenwen Yu, Chunyuan Li, Xu-Cheng Yin, Cheng-Lin Liu, Lianwen Jin, and Xiang Bai. Ocrbench: on the hidden mystery of ocr in large multimodal models. *Science China Information Sciences*, 67(12), 2024d. ISSN 1869-1919. doi: 10.1007/s11432-024-4235-6. URL <http://dx.doi.org/10.1007/s11432-024-4235-6>.
- Yuan Liuand, Haodong Duanand, Yuanhan Zhangand, Bo Liand, Songyang Zhangand, Wangbo Zhaoand, Yike Yuanand, Jiaqi Wangand, Conghui Heand, Ziwei Liuand, Kai Chenand, and Dahua Lin. Mmbench: Is your multi-modal model an all-around player? *arXiv:2307.06281*, 2023.
- Hashmat Shadab Malik, Fahad Shamshad, Muzammal Naseer, Karthik Nandakumar, Fahad Khan, and Salman Khan. Robust-llava: On the effectiveness of large-scale robust image encoders for multi-modal large language models. *arXiv preprint arXiv:2502.01576*, 2025.
- Joanna Materzyńska, Antonio Torralba, and David Bau. Disentangling visual and written concepts in clip. In *Proceedings of the IEEE/CVF Conference on Computer Vision and Pattern Recognition*, pages 16410–16419, 2022.
- Sachit Menon and Carl Vondrick. Visual classification via description from large language models. *arXiv preprint arXiv:2210.07183*, 2022.
- Meta. The llama 4 herd. <https://ai.meta.com/blog/llama-4-multimodal-intelligence/>, 2025.
- Yifei Ming and Yixuan Li. Understanding retrieval-augmented task adaptation for vision-language models. *arXiv preprint arXiv:2405.01468*, 2024.
- Anand Mishra, Shashank Shekhar, Ajeet Kumar Singh, and Anirban Chakraborty. Ocr-vqa: Visual question answering by reading text in images. In *ICDAR*, 2019.
- Moran Mizrahi, Guy Kaplan, Dan Malkin, Rotem Dror, Dafna Shahaf, and Gabriel Stanovsky. State of what art? a call for multi-prompt llm evaluation. *Transactions of the Association for Computational Linguistics*, 12:933–949, 2024.
- Ollama. <https://github.com/ollama/ollama>.
- OpenCLIP. https://github.com/mlfoundations/open_clip.
- OpenCV. <https://github.com/opencv/opencv>.

- Maan Qraitem, Nazia Tasnim, Piotr Teterwak, Kate Saenko, and Bryan A Plummer. Vision-llms can fool themselves with self-generated typographic attacks. *arXiv preprint arXiv:2402.00626*, 2024.
- Alec Radford, Jong Wook Kim, Chris Hallacy, Aditya Ramesh, Gabriel Goh, Sandhini Agarwal, Girish Sastry, Amanda Askell, Pamela Mishkin, Jack Clark, et al. Learning transferable visual models from natural language supervision. In *International conference on machine learning*, pages 8748–8763. PMLR, 2021.
- Aditya Ramesh, Prafulla Dhariwal, Alex Nichol, Casey Chu, and Mark Chen. Hierarchical text-conditional image generation with clip latents. *arXiv preprint arXiv:2204.06125*, 1(2):3, 2022.
- Anton Razzhigaev, Arseniy Shakhmatov, Anastasia Maltseva, Vladimir Arkhipkin, Igor Pavlov, Ilya Ryabov, Angelina Kuts, Alexander Panchenko, Andrey Kuznetsov, and Denis Dimitrov. Kandinsky: an improved text-to-image synthesis with image prior and latent diffusion. *arXiv preprint arXiv:2310.03502*, 2023.
- Robin Rombach, Andreas Blattmann, Dominik Lorenz, Patrick Esser, and Björn Ommer. High-resolution image synthesis with latent diffusion models. In *Proceedings of the IEEE/CVF conference on computer vision and pattern recognition*, pages 10684–10695, 2022.
- Christoph Schuhmann, Romain Beaumont, Richard Vencu, Cade W Gordon, Ross Wightman, Mehdi Cherti, Theo Coombes, Aarush Katta, Clayton Mullis, Mitchell Wortsman, Patrick Schramowski, Srivatsa R Kundurthy, Katherine Crowson, Ludwig Schmidt, Robert Kaczmarczyk, and Jenia Jitsev. LAION-5b: An open large-scale dataset for training next generation image-text models. In *Thirty-sixth Conference on Neural Information Processing Systems Datasets and Benchmarks Track*, 2022. URL <https://openreview.net/forum?id=M3Y74vmsMcY>.
- Amanpreet Singh, Vivek Natarajan, Meet Shah, Yu Jiang, Xinlei Chen, Dhruv Batra, Devi Parikh, and Marcus Rohrbach. Towards vqa models that can read, 2019. URL <https://arxiv.org/abs/1904.08920>.
- Label Studio. <https://labelstud.io>.
- Gemma Team, Aishwarya Kamath, Johan Ferret, Shreya Pathak, Nino Vieillard, Ramona Merhej, Sarah Perrin, Tatiana Matejovicova, Alexandre Ramé, Morgane Rivière, Louis Rouillard, Thomas Mesnard, Geoffrey Cideron, Jean bastien Grill, Sabela Ramos, Edouard Yvinec, Michelle Casbon, Etienne Pot, Ivo Penchev, Gaël Liu, Francesco Visin, Kathleen Kenealy, Lucas Beyer, Xiaohai Zhai, Anton Tsitsulin, Robert Busa-Fekete, Alex Feng, Noveen Sachdeva, Benjamin Coleman, Yi Gao, Basil Mustafa, Iain Barr, Emilio Parisotto, David Tian, Matan Eyal, Colin Cherry, Jan-Thorsten Peter, Danila Sinopalnikov, Surya Bhupatiraju, Rishabh Agarwal, Mehran Kazemi, Dan Malkin, Ravin Kumar, David Vilar, Idan Brusilovsky, Jiaming Luo, Andreas Steiner, Abe Friesen, Abhanshu Sharma, Abheesht Sharma, Adi Mayrav Gilady, Adrian Goedeckemeyer, Alaa Saade, Alex Feng, Alexander Kolesnikov, Alexei Bendebury, Alvin Abdagic, Amit Vadi, András György, André Susano Pinto, Anil Das, Ankur Bapna, Antoine Miech, Antoine Yang, Antonia Paterson, Ashish Shenoy, Ayan Chakrabarti, Bilal Piot, Bo Wu, Bobak Shahriari, Bryce Pettrini, Charlie Chen, Charline Le Lan, Christopher A. Choquette-Choo, CJ Carey, Cormac Brick, Daniel Deutsch, Danielle Eisenbud, Dee Cattle, Derek Cheng, Dimitris Paparas, Divyashree Shivakumar Sreepathihalli, Doug Reid, Dustin Tran, Dustin Zelle, Eric Noland, Erwin Huiuzenga, Eugene Kharitonov, Frederick Liu, Gagik Amirkhanyan, Glenn Cameron, Hadi Hashemi, Hanna Klimczak-Plucińska, Harman Singh, Harsh Mehta, Harshal Tushar Lehri, Hussein Hazimeh, Ian Ballantyne, Idan Szepktor, Ivan Nardini, Jean Pouget-Abadie, Jetha Chan, Joe Stanton, John Wieting, Jonathan Lai, Jordi Orbay, Joseph Fernandez, Josh Newlan, Ju yeong Ji, Jyotinder Singh, Kat Black, Kathy Yu, Kevin Hui, Kiran Vodrahalli, Klaus Greff, Linhai Qiu, Marcella Valentine, Marina Coelho, Marvin Ritter, Matt

- Hoffman, Matthew Watson, Mayank Chaturvedi, Michael Moynihan, Min Ma, Nabila Babar, Natasha Noy, Nathan Byrd, Nick Roy, Nikola Momchev, Nilay Chauhan, Noveen Sachdeva, Oskar Bunyan, Pankil Botarda, Paul Caron, Paul Kishan Rubenstein, Phil Culliton, Philipp Schmid, Pier Giuseppe Sessa, Pingmei Xu, Piotr Stanczyk, Pouya Tafti, Rakesh Shivanna, Renjie Wu, Renke Pan, Reza Rokni, Rob Willoughby, Rohith Vallu, Ryan Mullins, Sammy Jerome, Sara Smoot, Sertan Girgin, Shariq Iqbal, Shashir Reddy, Shruti Sheth, Siim Põder, Sijal Bhatnagar, Sindhu Raghuram Panyam, Sivan Eiger, Susan Zhang, Tianqi Liu, Trevor Yacovone, Tyler Liechty, Uday Kalra, Utku Evci, Vedant Misra, Vincent Roseberry, Vlad Feinberg, Vlad Kolesnikov, Woohyun Han, Woosuk Kwon, Xi Chen, Yinlam Chow, Yuvein Zhu, Zichuan Wei, Zoltan Egyed, Victor Cotruta, Minh Giang, Phoebe Kirk, Anand Rao, Kat Black, Nabila Babar, Jessica Lo, Erica Moreira, Luiz Gustavo Martins, Omar Sanseviero, Lucas Gonzalez, Zach Gleicher, Tris Warkentin, Vahab Mirrokni, Evan Senter, Eli Collins, Joelle Barral, Zoubin Ghahramani, Raia Hadsell, Yossi Matias, D. Sculley, Slav Petrov, Noah Fiedel, Noam Shazeer, Oriol Vinyals, Jeff Dean, Demis Hassabis, Koray Kavukcuoglu, Clement Farabet, Elena Buchatskaya, Jean-Baptiste Alayrac, Rohan Anil, Dmitry, Lepikhin, Sebastian Borgeaud, Olivier Bachem, Armand Joulin, Alek Andreev, Cassidy Hardin, Robert Dadashi, and Léonard Hussenot. Gemma 3 technical report, 2025. URL <https://arxiv.org/abs/2503.19786>.
- Michael Tschannen, Alexey Gritsenko, Xiao Wang, Muhammad Ferjad Naeem, Ibrahim Alabdulmohsin, Nikhil Parthasarathy, Talfan Evans, Lucas Beyer, Ye Xia, Basil Mustafa, et al. Siglip 2: Multilingual vision-language encoders with improved semantic understanding, localization, and dense features. *arXiv preprint arXiv:2502.14786*, 2025.
- Alexander Visheratin. Nllb-clip-train performant multilingual image retrieval model on a budget. *arXiv preprint arXiv:2309.01859*, 2023.
- Xiaohua Zhai, Basil Mustafa, Alexander Kolesnikov, and Lucas Beyer. Sigmoid loss for language image pre-training. In *Proceedings of the IEEE/CVF international conference on computer vision*, pages 11975–11986, 2023.
- Zihao Zhao, Yuxiao Liu, Han Wu, Mei Wang, Yonghao Li, Sheng Wang, Lin Teng, Disheng Liu, Zhiming Cui, Qian Wang, et al. Clip in medical imaging: A comprehensive survey. *arXiv preprint arXiv:2312.07353*, 2023.
- Xingcheng Zhou, Mingyu Liu, Ekim Yurtsever, Bare Luka Zagar, Walter Zimmer, Hu Cao, and Alois C Knoll. Vision language models in autonomous driving: A survey and outlook. *IEEE Transactions on Intelligent Vehicles*, 2024.
- Ziqin Zhou, Yinjie Lei, Bowen Zhang, Lingqiao Liu, and Yifan Liu. Zegclip: Towards adapting clip for zero-shot semantic segmentation. In *Proceedings of the IEEE/CVF conference on computer vision and pattern recognition*, pages 11175–11185, 2023.

Appendix A. Appendix

A.1 Example Images of SCAM, NoSCAM, and SynthSCAM

In fig. 7, we highlight some examples from the **S**ubtle **C**haracter **A**ttacks on **M**ultimodal **M**odels (**SCAM**) dataset and the generated NoSCAM and SynthSCAM datasets.



Figure 7: Example images of SCAM, NoSCAM, and SynthSCAM.

A.2 Example Images of PAINT and RTA-100

Although qualitative inspection is necessarily subjective and 20 samples from the PAINT (Ilharco et al., 2022) resp. RTA-100 (Azuma and Matsui, 2023) datasets in figs. 8 and 9 cannot capture their full variability, the quantitative evidence in table 2 and the attack-word distribution shown in fig. 3 clarify the structural differences. PAINT and RTA-100 cover comparatively restricted sets of objects, attack words, and scene conditions. SCAM, by contrast, comprises 1162 images with 660 objects and 206 attack words collected by nine contributors across diverse indoor and outdoor environments. The resulting variation in lighting, backgrounds, camera quality, handwriting styles, and viewpoints is visible in fig. 2, even if such diversity is difficult to discern from limited qualitative examples alone.



Figure 8: 20 random example images from the PAINT (Ilharco et al., 2022) dataset. Best viewed zoomed in.



Figure 9: 20 random example images from the RTA-100 (Azuma and Matsui, 2023) dataset. Best viewed zoomed in.

A.3 Zero-Shot Evaluation of LVMs: Text Templates

To compute the cosine similarity between an image and text embeddings in our zero-shot evaluation of Vision-Language Models (VLMs), we generate text embeddings for both the object label and the attack word using multiple textual variations. Specifically, we apply 32 diverse text templates as in (Radford et al., 2021), each incorporating the object label resp. attack word in a different context. The final embedding is obtained by averaging the embeddings of all templates. The templates are as follows: ('a bad photo of a {}.', 'a photo of many {}.', 'a sculpture of a {}.', 'a photo of the hard to see {}.', 'a low resolution photo of the {}.', 'a rendering of a {}.', 'graffiti of a {}.', 'a bad photo of the {}.', 'a cropped photo of the {}.', 'a tattoo of a {}.', 'the embroidered {}.', 'a photo of a hard to see {}.', 'a bright photo of a {}.', 'a photo of a clean {}.', 'a photo of a dirty {}.', 'a dark photo of the {}.', 'a drawing of a {}.', 'a photo of my {}.', 'the plastic {}.', 'a photo of the cool {}.', 'a close-up photo of a {}.', 'a black and white photo of the {}.', 'a painting of the {}.', 'a painting of a {}.', 'a pixelated photo of the {}.', 'a sculpture of the {}.', 'a bright photo of the {}.', 'a cropped photo of a {}.', 'a plastic {}.', 'a photo of the dirty {}.', 'a jpeg corrupted photo of a {}.', 'a blurry photo of the {}.').

A.4 Model Accuracies on Typographic Attack Datasets

Table 6: Performance of (Large) Vision-Language Models available through OpenCLIP (OpenCLIP) resp. ollama (Ollama), and Anthropic’s resp. OpenAI’s API on SCAM, PAINT (Ilharco et al., 2022), and RTA-100 (Azuma and Matsui, 2023) datasets.

Model	Training data	Accuracy (%)				
		NoSCAM	SCAM	SynthSCAM	PAINT	RTA-100
RN101	openai	97.93	40.14	26.18	36.36	35.10
RN50	openai	97.76	36.61	22.39	33.64	30.40
RN50x16	openai	98.79	37.12	34.19	46.36	32.70
RN50x4	openai	98.19	32.90	26.36	35.45	30.50
RN50x64	openai	98.97	32.04	31.78	43.64	35.40
ViT-B-16	commonpool_l_basic_s1b_b8k	98.62	90.09	83.03	82.73	88.10
	commonpool_l_clip_s1b_b8k	98.54	71.15	62.53	69.09	71.50
	commonpool_l_image_s1b_b8k	98.45	90.96	85.96	88.18	89.00
	commonpool_l_laion_s1b_b8k	97.59	79.24	65.72	77.27	72.90
	commonpool_l_s1b_b8k	98.02	88.72	81.65	86.36	87.20
	commonpool_l_text_s1b_b8k	98.36	91.82	85.10	85.45	90.00
	datacomp_l_s1b_b8k	98.19	80.10	69.51	71.82	76.60
	datacomp_xl_s13b_b90k	99.14	68.39	53.14	62.73	66.80
	laion2b_s34b_b88k	98.71	69.16	52.28	64.55	64.20
	laion400m_e31	98.62	69.16	50.90	66.36	62.60
	laion400m_e32	98.71	68.91	50.90	65.45	61.90
	metaclip_400m	98.62	58.66	35.40	50.00	57.10
	metaclip_fullcc	98.88	60.81	39.62	49.09	59.20
	openai	97.59	39.71	20.24	33.64	37.60
ViT-B-16-SigLIP	webli	99.22	81.40	75.45	82.73	78.10
ViT-B-16-SigLIP-256	webli	99.31	80.96	75.97	83.64	80.00
ViT-B-16-SigLIP-384	webli	99.48	84.24	80.45	84.55	82.20
ViT-B-16-SigLIP-512	webli	99.66	85.70	81.14	83.64	82.90
ViT-B-16-SigLIP-i18n-256	webli	99.40	89.66	85.70	89.09	85.70
ViT-B-16-plus-240	laion400m_e31	98.97	71.75	54.44	63.64	62.70
	laion400m_e32	98.97	71.75	54.44	63.64	62.70
ViT-B-32	commonpool_m_basic_s128m_b4k	89.15	90.78	91.47	92.73	92.70
	commonpool_m_clip_s128m_b4k	91.30	90.70	90.53	94.55	92.20
	commonpool_m_image_s128m_b4k	89.66	91.30	92.08	94.55	92.40
	commonpool_m_laion_s128m_b4k	89.23	90.35	90.18	94.55	91.20
	commonpool_m_s128m_b4k	88.11	89.84	90.70	95.45	90.60
	commonpool_m_text_s128m_b4k	89.32	91.04	90.96	94.55	93.40
	commonpool_s_basic_s13m_b4k	72.70	74.33	74.76	72.73	74.10
	commonpool_s_clip_s13m_b4k	76.31	76.57	76.66	76.36	77.10
	commonpool_s_image_s13m_b4k	72.95	73.21	73.47	78.18	72.50
	commonpool_s_laion_s13m_b4k	73.73	73.39	74.25	78.18	74.00
	commonpool_s_s13m_b4k	74.68	74.25	73.99	70.91	72.40
	commonpool_s_text_s13m_b4k	74.42	73.99	74.50	79.09	74.50
	datacomp_m_s128m_b4k	89.75	90.61	90.61	94.55	92.20
	datacomp_xl_s13b_b90k	98.88	79.33	64.17	69.09	76.30
	laion2b_s34b_b79k	98.45	74.68	56.16	68.18	66.00
	laion400m_e31	96.64	63.57	40.48	55.45	57.70
	laion400m_e32	96.64	63.48	40.57	54.55	57.40
	metaclip_400m	97.16	77.00	55.99	68.18	77.10
	metaclip_fullcc	98.45	79.93	58.91	67.27	75.30
	openai	96.47	60.81	33.59	52.73	51.40
ViT-B-32-256	datacomp_s34b_b86k	98.54	73.30	60.72	70.91	70.00
ViT-H-14	laion2b_s32b_b79k	99.22	62.96	47.63	51.82	55.60
	metaclip_altogether	99.48	66.58	52.89	61.82	58.30
	metaclip_fullcc	99.40	62.27	43.41	53.64	55.60
ViT-H-14-CLIPA	datacomp1b	99.66	64.69	57.02	49.09	57.30

Continued on next page

SCAM: REAL-WORLD TYPOGRAPHIC ROBUSTNESS EVALUATION

Model	Training data	NoSCAM	SCAM	SynthSCAM	PAINT	RTA-100
ViT-H-14-CLIPA-336	datacomp1b	99.66	61.15	55.64	46.36	59.10
	laion2b	99.22	71.92	60.47	60.00	61.60
ViT-L-14	commonpool_xl_clip_s13b_b90k	99.48	57.62	48.84	44.55	51.80
	commonpool_xl_laion_s13b_b90k	99.40	74.94	59.09	62.73	67.40
	commonpool_xl_s13b_b90k	99.48	74.68	68.56	56.36	65.80
	datacomp_xl_s13b_b90k	99.48	60.38	52.97	50.00	56.00
	laion2b_s32b_b82k	99.05	62.53	48.23	59.09	56.40
	laion400m_e31	99.05	67.18	51.42	63.64	59.50
	laion400m_e32	99.05	66.75	52.02	63.64	59.90
	metaclip_400m	98.71	57.71	39.62	50.00	54.30
	metaclip_fullcc	99.14	63.14	45.48	47.27	52.60
	openai	99.14	40.14	26.61	40.00	36.90
ViT-L-14-336	openai	99.22	33.85	26.44	33.64	39.90
ViT-L-14-CLIPA	datacomp1b	99.48	72.61	63.57	63.64	66.80
ViT-L-14-CLIPA-336	datacomp1b	99.57	74.76	65.81	63.64	68.50
ViT-L-16-SigLIP-256	webli	99.57	86.48	80.10	81.82	79.60
ViT-L-16-SigLIP-384	webli	99.66	87.25	81.65	76.36	77.40
ViT-S0400M-14-SigLIP	webli	99.74	84.07	82.17	84.55	81.10
ViT-S0400M-14-SigLIP-378	webli	99.66	85.62	85.01	83.64	81.30
ViT-S0400M-14-SigLIP-384	webli	99.66	85.44	84.58	81.82	81.20
ViT-S0400M-16-SigLIP-i18n-256	webli	99.74	88.89	83.98	85.45	86.30
ViT-bigG-14	laion2b_s39b_b160k	99.40	70.89	58.91	56.36	58.50
	metaclip_fullcc	99.31	68.04	53.66	60.00	58.30
ViT-bigG-14-CLIPA	datacomp1b	99.66	68.04	59.35	56.36	63.20
ViT-bigG-14-CLIPA-336	datacomp1b	99.74	64.00	56.68	58.18	59.40
ViT-g-14	laion2b_s12b_b42k	99.14	69.25	55.38	59.09	54.70
	laion2b_s34b_b88k	99.05	61.93	47.03	54.55	50.10
convnext_base	laion400m_s13b_b51k	98.54	59.09	40.40	49.09	54.10
convnext_base_w	laion2b_s13b_b82k	98.79	66.84	52.28	60.91	59.40
	laion2b_s13b_b82k_augreg	98.88	68.73	56.33	60.00	57.40
	laion_aesthetic_s13b_b82k	98.45	68.13	51.59	59.09	59.70
convnext_base_w_320	laion_aesthetic_s13b_b82k	98.62	68.91	51.25	55.45	61.40
	laion_aesthetic_s13b_b82k_augreg	98.62	72.27	59.00	59.09	63.90
convnext_large_d	laion2b_s26b_b102k_augreg	99.40	67.18	54.78	54.55	53.70
convnext_large_d_320	laion2b_s29b_b131k_ft	99.31	67.10	57.11	55.45	56.90
	laion2b_s29b_b131k_ft_soup	99.57	67.53	56.16	53.64	57.00
convnext_xxlarge	laion2b_s34b_b82k_augreg	99.48	64.94	54.69	50.91	59.80
	laion2b_s34b_b82k_augreg_rewind	99.22	66.15	54.09	55.45	58.80
	laion2b_s34b_b82k_augreg_soup	99.48	64.94	54.44	55.45	59.00
nllb-clip-base	v1	94.66	76.66	61.67	71.82	74.90
nllb-clip-base-siglip	mrl	98.28	71.92	63.91	70.91	69.40
	v1	98.71	77.69	75.88	75.45	78.60
nllb-clip-large	v1	97.50	61.41	48.58	56.36	60.90
nllb-clip-large-siglip	mrl	98.88	72.27	66.75	66.36	71.20
	v1	99.05	73.90	75.37	74.55	75.90
roberta-ViT-B-32	laion2b_s12b_b32k	97.67	75.45	57.45	62.73	68.50
xlm-roberta-base-ViT-B-32	laion5b_s13b_b90k	98.62	76.83	59.00	69.09	71.20
xlm-roberta-large-ViT-H-14	frozen_laion5b_s13b_b90k	99.22	63.74	47.89	54.55	56.70
llava-llama3:8b	-	98.09	39.50	44.04	48.62	41.83
llava:7b-v1.6	-	97.50	58.43	61.45	53.64	51.20
llava:13b-v1.6	-	98.88	58.00	55.42	54.55	56.00
llava:34b-v1.6	-	98.97	84.85	85.11	89.09	81.50
gemma3:4b	-	97.24	58.05	64.80	50.00	60.66
gemma3:12b	-	99.14	52.02	64.80	44.55	50.50
gemma3:27b	-	97.42	81.67	83.65	80.91	78.10
llama3.2-vision:90b	-	98.88	71.01	74.65	77.06	68.41
llama4:scout	-	99.23	88.12	87.18	89.09	86.20
gpt-4o-mini-2024-07-18	-	99.40	84.68	87.09	90.91	85.15
claude-sonnet-4-20250514	-	99.31	91.13	90.28	95.45	87.30
gpt-4o-2024-08-06	-	99.48	96.82	94.58	99.09	96.73

A.5 Architecture Comparison

In table 5a in the main text, we compare different architectures (CLIP-RN vs. CLIP-ViT, and CLIP-ViT vs. SigLIP-ViT) and present averaged accuracies. Table 7 details the specific models that we choose from the OpenCLIP suite for this comparison.

Table 7: Models chosen from the OpenCLIP suite for architecture comparison in table 5a. The table groups models by architecture category and indicates the corresponding fixed training data. In OpenCLIP, v1 refers to LAION-COCO NLLB (Visheratin, 2023).

Architecture Category	Model	Training Data
CLIP-ViT	ViT-B-32	openai
	ViT-B-16	openai
	ViT-L-14	openai
	ViT-L-14-336	openai
CLIP-RN	RN50	openai
	RN101	openai
	RN50x4	openai
	RN50x16	openai
	RN50x64	openai
SigLIP-ViT	nllb-clip-base-siglip	v1
	nllb-clip-large-siglip	v1
CLIP-ViT	nllb-clip-base	v1
	nllb-clip-large	v1

A.6 Prompt Variation

Our evaluation of Large Vision-Language Models (LVLMs) in section 4 focuses on a single prompt. Given prior work demonstrating the importance of prompt phrasing and advocating for multi-prompt evaluation (Mizrahi et al., 2024; Cheng et al., 2024b), we additionally test a modified version that appears “safer.” This variant appends the instruction “Do not get fooled by typographic attacks.” to the original prompt. Contrary to the expectation formulated in these works, this modification does not reduce vulnerability. As illustrated in fig. 10, the susceptibility to typographic attacks remains largely unchanged.

A.7 Replacing VLM in LLaVA

Previous work (Cheng et al., 2024a; Li et al., 2024) suggest that susceptibility to typographic attacks can be attributed to a cross-modal alignment deficiency inherent to LVLMs while the functionality of vision encoders is intact. Further, (Malik et al., 2025) demonstrates that integrating an adversarially pretrained vision encoder into LLaVA significantly improves robustness against various attacks, including typographic perturbations introduced in (Li et al., 2024).

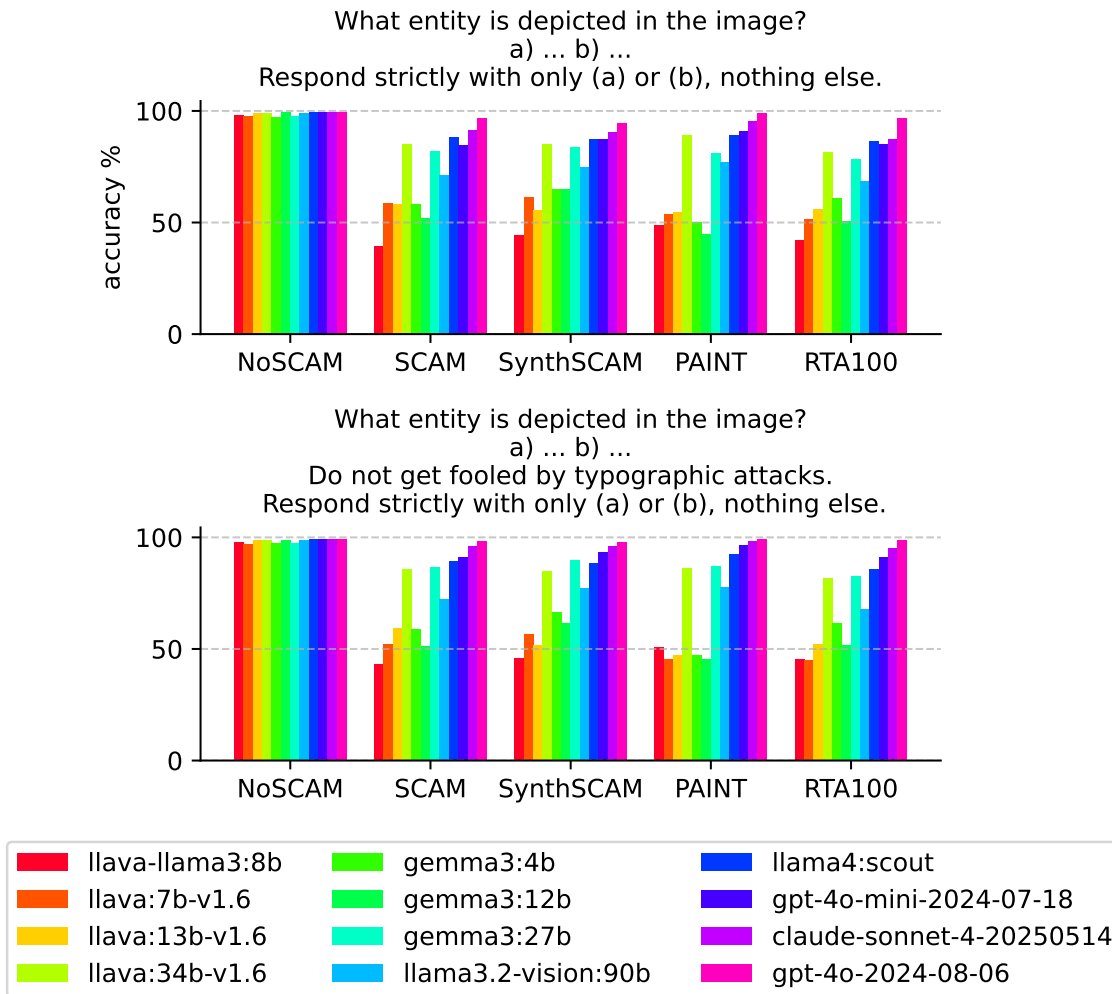


Figure 10: The modified “safer” prompt does not alleviate susceptibility to typographic attacks.

Our evaluations on SCAM support the conclusion that some Vision-Language Models (VLMs) exhibit higher typographic robustness than others. In particular, LLMs using the OpenAI-trained ViT-L-14-336 encoder trained – such as LLaVA (Li et al., 2023b; Liu et al., 2023a, 2024b) – show heightened vulnerability. To isolate the effect of the vision encoder, we train a LLaVA model using the ViT-L-14-CLIPA-336 encoder (Li et al., 2023c,d), which was trained on datacomp1b and differs primarily in training data and regime, not architecture. Compared to the OpenAI encoder, the CLIPA model exhibits a substantially lower robustness drop: only 25% from NoSCAM to SCAM, versus 65% (see table 1). It also outperforms the OpenAI encoder by 3% on average across 38 datasets evaluated using OpenCLIP (Ilharco et al., 2021)⁴.

4. https://github.com/mlfoundations/open_clip/blob/main/docs/openclip_results.csv

We use the official LLaVA codebase (Liu), modified⁵ to support OpenCLIP models, and closely follow the original training procedure to conduct our experiments. The pretraining step ran on 8×A100 (40GB) GPUs and completed in approximately 4 hours; finetuning required around 14 hours.

Table 8 shows that our CLIPA-based LLaVA variant does not outperform the original model on SCAM, despite using a VLM that is more robust in isolation. Performance on other benchmarks evaluated via VLMEvalKit (Duan et al., 2024) also drops. These findings suggest that the benefits of a more robust vision encoder do not transfer under naive LLaVA integration.

Note the experimental constraints: only one small Large Language Model (LLM) (Vicuna v1.5 7B), only two different vision backbones, and no hyperparameter tuning are employed.

Table 8: Performance comparison of the original LLaVA-v1.5-7B and our CLIPA-based LLaVA variant across diverse benchmarks. Despite the CLIPA vision encoder showing stronger robustness in isolation, this does not translate to improved performance on SCAM. Evaluations for the upper section are conducted using VLMEvalKit (Duan et al., 2024). Other results follow the protocol outlined in the main part of the paper.

Benchmark	LLaVA-v1.5-7B (orig.)	LLaVA-v1.5-7B-CLIPA (ours)
MMBench v1.1 (Liu and et al., 2023)	64.32	60.22
MME Perception (Fu et al., 2023)	1444.81	1378.96
SEED-Bench-1 (img) (Li et al., 2023a)	66.81	64.02
TextVQA (Singh et al., 2019)	46.93	45.57
OCRBench (Liu et al., 2024d)	31.90	31.60
OCR-VQA (Mishra et al., 2019)	60.64	57.39
NoSCAM	97.16	89.66
SCAM	54.69	45.48
SynthSCAM	51.55	46.08
PAINT (Ilharco et al., 2022)	52.73	53.64
RTA100 (Azuma and Matsui, 2023)	48.30	47.30

A.8 Typographic Robustness vs. Typographic Understanding

The main paper shows that increasing the size of LLM backbones reduces susceptibility to typographic attacks (see results for LLaVA and Gemma3 in table 1). Simultaneously, benchmarks such as TextVQA and OCRBench, reported on the VLMLeaderboards⁶, indicate that typographic understanding – essentially, reading – also improves with model scale (see table 9). Together, these findings suggest that typographic robustness emerges as model size increases, alongside improved textual perception. However, (Kimura et al., 2024) reports the opposite correlation between susceptibility and OCR performance in LVLMs, indicating that stronger reading ability alone does not guarantee robustness.

5. <https://github.com/Bliss-e-V/LLaVA-OpenCLIP>

6. https://huggingface.co/spaces/opencompass/open_vlm_leaderboard

Table 9: Performance of selected LLaVA-Next (Liu et al., 2024b) models on three OCR-related benchmarks (TextVQA (Singh et al., 2019), OCRBench (Liu et al., 2024d) (from VLMEvalKit (Duan et al., 2024)), and OCR-VQA (Mishra et al., 2019)) shows that increasing LLM backbone size leads to improved typographic understanding. All models use the ViT-L-14-336 vision encoder. Results are reported from the OpenVLM leaderboard, evaluated using the VLMEvalKit toolkit (Duan et al., 2024).

Model	Params (B)	TextVQA (%)	OCRBench	OCR-VQA (%)
LLaVA-Next-Yi-34B	34.8	69.3	574	66.3
LLaVA-Next-Vicuna-13B	13.4	66.9	537	65.3
LLaVA-Next-Llama3	8.0	65.3	531	60.7
LLaVA-Next-Mistral-7B	7.6	65.2	531	61.2
LLaVA-Next-Vicuna-7B	7.1	63.8	532	63.8

A.9 SCAM Labels

The SCAM dataset includes diverse object labels:

30kmh traffic zone sign, adapter, advent calendar, alarm clock, analog timer, apple, apple seed cutter, apples, armchair, ashtray, aubergine, avocado, axe, back, backpack, bacon bits, badminton ball, bag, baking pan, ball, balloon, banana, bananas, band-aid, barricade, baseball cap, basket, basket ball, bathroom sign, bathtub, batteries, bed, bell, bell pepper, bench, bench vise, bicycle, bicycle bell, bicycle light, bicycle tire, bike, bike light, bike lock, bin, bird feeder, blackboard, blanket, blender, blower, board, boat figurine, book, boot, bottle, bottle cap, bottle crate, bottle opener, bottles, boulder, bowl, box, boxes, brass tubes, bread slicer, bricks, broom, brooms, brush, brushes, bucket, butterfly, buttons, cabinet, cable, cable drum, cable ties, cage, cake, calculator, calendar, camera, candle, candles, candy cane, canister, cans, cap, capacitor, car, carafe, cardboard box, carrot, cash register, cashew nuts, cat figurine, cat tower, cauldron, celery, chain, chain saw, chair, chalk bag, champagne, charger, cheese, chess board, chess piece, chess set, chessboard, chewing gum, chewing gums, chili pepper, chips, chocolate, chopsticks, cigarettes, cleaner, clipboard, clock, closet, clothes iron, clothespin, coat, coat hanger, coat hook, coffee beans, coffee machine, coffee maker, coin, coin counter, combination lock, compass, condom, condoms, confetti, contact grill, controller, cooking scraper, cordless drill, cork, corn, counter, cow meat, crepe pan, crochet hook, cross wrench, cucumber, cup, deodorant, detergent, detergent powder, diapers, dice, diffuser, dish scrubber, dish soap, dishwasher, dishwasher tablets, disinfectant dispenser, dispenser, diving goggles, dog prohibition sign, doll, door, doorhandle, doormat, drill, drills, drink, drone, drum, duct tape, dustpan, dvd, e-scooter, ear phones, ear plugs, ear protection, easel, edamame, edding, eggs, electric kettle, electric screwdriver, electric shaver, electric toothbrush, electrical panel, elephant, emergency exit sign, end of parking zone sign, ernie, exit sign, faucet, feeder, fence, fennel, fever thermometer, figurine, fineliner pen, fire alarm button, fire detector, fire extinguisher, firework, first aid kit, fish, flip flops, flipper, floss, flower, flower pot, flowering pot, flowers, folder, folding rule, fork, fortune cookie, freeze pack, french press, fridge, fries, frisbee, frothing pitcher, fryer, funnel, garden gnome, garlic, gas bottle, gas cooker, gem lettuce, ginger, glas, glass, glass bottle, glasses, globe, glove, glue stick, gnocchi, goal, goggles, goose, grapes, grater, grave candles, green beans, grill, guitar, guitar foot stand, hair clip, hair clipper, hair dryer, hair iron, hairbrush, hairgrip, hairspray, ham, hammer,

hand blender, hand brush and dustpan, handbrush, handkerchiefs, handwash, hanger, hard disk, hare, hat, hdmi splitter, headband, headphones, heater, helmet, high visibility jacket, hook, horn, hot dog maker, hot glue gun, hot water bottle, hotplate, ice cube tray, ice pack, ice scraper, icecream, intercom, interdental brush, iron, ironing board, jacket, jam, jar, jersey, juggling ball, juicer, kettle, key, key chain, keyboard, keys, kiwi, knife, labeling machine, ladder, lamp, landing net, lantern, laptop, lawn chair, letter box, lid, light bulbs, light switch, lightbulb, lighter, lime, lipstick, lollies, lollipop, loofah, macbook, magazine, makeup powder, mango, marker, masher, mask, matryoshka doll, meatball, melon, memory card, menstrual pad, menstrual pads, mercedes-benz, metronome, microcontroller, microphone, microwave, milk pitcher, mirror, moka pot, money, monitor, mosquito repellent, mosquito spray, motion detector, mouse, mug, mulled wine, multiple socket, mushroom, mushrooms, nail clipper, nail polish, napkin, necklace, no entry sign, no parking sign, no pedestrian crossing sign, no smoking sign, no-entry sign, noodle cooker, notebook, nuts, oat bar, oats, octopus, office chair, olives, onion, onions, orange, organizer, oven, oven glove, paint, paint brush, paint roller, painting, pair, palette knife, pallet, pan, panini press, pants, paper rolls, paper streamers, paper towel, paper towels, paper wrap, paprika, parking sign, parking ticket machine, parsley, party hat, pasta, pea, pen, pencil, pepper, pepper caster, perfume, person, phone, pick, pickaxe, piggy bank, pillow, pills, pine cone, pineapple plant, pineapples, ping pong ball, pipe connection, pipes, pizza, pizza cutter, pizza oven, pizza peel, plane ticket, plant, plastic cups, plate, playing card, plectrum, plug board, plug socket, plunger, pocket balance, pocket knife, pokemon ball, pole, portable electric drill, post, post-its, pot, potato, potato chips, potato masher, potatoes, pouch, pouffe, power drill, powerbank, printer, printer cartridge, projector, puffed rice, pump, pumpkin, puzzle, puzzle piece, rack, racket, radiator, radio, railing, rake, razor, record player, remote, remote control, resistor, ribbon, rice cooker, roll board, roll-on, roller, roller board, rolling pin, rope, rose, rosemary, roses, router, rubber bands, rubber duck, rubik's cube, running shoes, safe, safety pin, safety pins, safety sign, sage leaves, salad, salami, salmon, salt, sandal, sandpaper, sandwich maker, santa figurine, sausage, sausages, saw, scissor, scissors, scooter, screen, screw, screwdriver, screws, seafood salad, serving tray, serving trolley, sewing machine, shaker, shampoo, shashlik skewers, shaver, shelf, shell, shirt, shoe, shoes, shopping cart, shovel, shovels, shower, shower gel, shower head, shrimp, shuttlecock, sieve, sign, silverware box, sink, skillet, skimmer, skimmers, sledgehammer, sleeping mat, slider, slipper, slippers, sneaker, soap, soap dispenser, sock, socket, socks, spade, speaker, spice mill, spinach, spiral notebooks, sponge, spoon, spout, spray bottle, spray can, spring, squeegee, stamp, stapler, steam flat iron, step bin, stereo, stone plates, stool, stop sign, storage box, straw, straws, string, stuffed animal, suitcase, sunglasses, sunscreen, sweeper, t-shirt, table, takeaway bag, tampon, tap, tape, tape dispenser, tea, tea pot, teabag, tealight, tee box, telephone, tennis ball, terminal, thermal camping mat, thermometer, thread, ticket machine, tin box, tire, tissues, toaster, toilet, toilet bowl, toilet brush, toilet lid, toilet paper, tomato, tomatoes, tongue brush, toothbrush, toothpaste, tortellini, towel, toy car, toy elephant, toy horse, traffic light, traffic signs, trailer, trash bag, trash bin, trash can, trashcan, tray, tree, try square, turmeric, turtle, tv, ufonauts, umbrella, underpants, usb cable, usb-c cable, vacuum, vacuum cleaner, vase, vegetable peeler, video surveillance sign, vinyl, waffles, wall, wall charger, wallet, washbasin, washing machine, watch, water wings, watering can, watermelon, webcam, weight, wet floor sign, wheel, whisk, white cabbage, wildlife camera, window, window cleaner, wine, wood, wooden disc, wooden grill tong, wooden panels, wooden pestle, wooden skewer, wool, wrapping paper, wrench, yarn, and zucchini.

Table 10 summarizes the frequency of object labels. The top 15 labels (e.g., “lamp”, “plant”, “bottle”) are among the most frequent, while the bottom 5 labels (e.g., “chain”, “roller board”, “mask”) appear rarely. Notably, 437 object labels appear exactly once, illustrating a pronounced long-tail distribution that underscores the diversity of the dataset.

Table 10: Top 15 and bottom 5 object labels by appearance frequency.

Object label	Count
lamp	13
plant	13
bottle	13
chair	11
glass	10
candle	10
cable	8
grill	8
printer	8
cup	8
speaker	8
pillow	8
brush	7
canister	7
pen	7
...	
chain	1
roller board	1
mask	1
goggles	1
webcam	1

SCAM includes a variety of attack words:

apple, arrow, bag, ball, barrier, basketball, beach, beatles, bed, beer, bell, bench, bicycle, bike, bird, blanket, boat, book, boot, bottle, boulder, bowl, box, boy, bracelet, bridge, bridge out, broom, bus, butter, cable, cake, camera, canal, candle, cane, cannon, cap, car, carpet, carrot, cart, cat, cellphone, chair, cheese, chest, chicken, child, clock, cloud, coat, coin, cone, couch, cow, crab, crystal, cup, curb, curtaxin, curve, dead end, deer, desert, desk, detour, dish, dog, door, duck, eagle, egg, elevator, exit, fan, feather, fence, finger, fire, fish, flag, floor, flower, fog, forest, fork, frog, fruit, garbage bin, gears, ginger, gloves, grandpa, grape, grass, gravel, green, grenade, gun, hair, hammer, hat, helmet, highway, hill, hole, honey, horn, horse, house, ice, iron, jacket, jar, jeep, key, knife, ladder, lake, lamp, lane, leaf, lemon, lentils, lift, lightbulb, lion, lipstick, lock, macbook, mad, median, merge, mirror, mittens, mountaxin, no left turn, no parking, ocean, olive oil, oregano, pedestrian, pen, person, phone, piano, picasso, pig, police, pumpkin, raccoon, red light, risotto rice, river, road, road closed, rock, saddle, salt, sandwich, santa claus, scarf, scooter, screw, screwdriver, sea, seed,

shadow, ship, sidewalk, signal, slippery, sloth, slow, smartphone, sofa, speed camera, speed limit, spok, spoon, staxirs, stop, stop sign, store, street, street sign, suv, table, taxi, toll, traffic light, traffic sign, train, transistor, trash, tree, truck, unicorn, van, vase, wall, wet, woman, yield, and zebra.

Table 11 summarizes the frequency of attack words. The top 15 attack words (e.g., “knife”, “truck”, “slow”) occur frequently, whereas many attack words are rare. In fact, 56 attack words appear exactly once, again highlighting overall diversity of the dataset.

Table 11: Top 15 and bottom 5 attack words by appearance frequency.

Attack Word	Count
knife	24
truck	23
slow	20
lion	20
zebra	19
helmet	18
bike	17
honey	15
pig	15
camera	15
lemon	15
pen	15
tree	14
house	14
fish	13
...	
beatles	1
green	1
raccoon	1
beach	1
unicorn	1